ORGINAL ARTICLE

Non-Invasive Determination of Blood Glucose Levels by Optical Waveguide

Mohsen Askarbioki[1], Mojtaba Mortazavi[1], Abdolhamid Amooee[2*], Saeid Kargar[2], Mohammad Afkhami-Ardekani[3], Seyed Pezhman Shirmardi[1], Reihane Ranjbar Jamalabadi[4]

1. Nuclear Science and Technology Research Institute (NSTRI), Tehran, Iran.
2. Department of General Surgery, Shahid Sadoughi University of Medical Sciences, Yazd, Iran.
3. Diabetes Research Center, Shahid Sadoughi University of Medical Sciences Yazd, Iran.
4. Depatment of Pediatrics, School of Medicine, Shahid Sadoughi University of Medical Sciences, Yazd, Iran.

***Correspondence:**
Abdolhamid Amooee, Department of General Surgery, Shahid Sadoughi University of Medical Sciences, Yazd, Iran.
Tel: (98) 913 152 9380
Email: ab.amooee@yahoo.com
ORCID ID: (0000-0002-0508-0957)

Received: 15 July 2021

Accepted: 06 October 2021

Published in November 2021

Abstract

Objective: Today, there are various non-invasive techniques available for the determination of blood glucose levels. In this study, the level of blood glucose was determined by developing a new device using near-infrared (NIR) wavelength, glass optical waveguide, and the phenomenon of evanescent waves.

Materials and Methods: The body's interstitial fluid has made possible the development of new technology to measure the blood glucose. As a result of contacting the fingertip with the body of the borehole rod, where electromagnetic waves are reflected inside, evanescent waves penetrate from the borehole into the skin and are absorbed by the interstitial fluid. The electromagnetic wave rate absorption at the end of the borehole rod is investigated using a detection photodetector, and its relationship to the people's actual blood glucose level.

Following precise optimization and design of the glucose monitoring device, a statistical population of 100 participants with a maximum blood glucose concentration of 200 mg/dL was chosen. Before measurements, participants put their index finger for 30 seconds on the device.

Results: According to this experimental study, the values measured by the innovative device with Clark grid analysis were clinically acceptable in scales A and B. The Adjusted Coefficient of Determination of the data was estimated to be 0.9064.

Conclusion: For future investigations, researchers are recommended to work with a larger statistical population and use error reduction trends to improve the accuracy and expand the range of measurements.

Keywords: Non-invasive measurement, Hollow beam, Detection sensitivity, Divergence angle, Probe rod

Introduction

Diabetes is a widely spread disease in both industrialized and developing countries (1). It is a chronic metabolic disorder that impacts vital organs of the body, where continuous monitoring of blood glucose concentration prevents further complications

[Downloaded from ijdo.ssu.ac.ir on 2026-11-20]

[DOI: 10.18502/ijdo.v13i4.8001]

(2). Researchers have continued to attempt to study a variety of techniques for measuring blood glucose concentration while emphasizing the accuracy of the measurements as a critical factor (3).

There are many articles about the classification of various methods of monitoring and controlling blood sugar. During the past three decades, many blood sugar monitoring and diet management technologies have been used and a variety of techniques have been compared. Blood glucose measurements are mainly classified into invasive, non-invasive, and minimally invasive methods, with the majority of studies that focus on the development of non-invasive measurements (4). Non-invasive sensors, however, measure other markers in addition to blood sugar (5). Such sensors are at the top of research to control blood sugar due to extensive investigation in diabetic patients (6).

Many companies are engaged in researching and developing commercialized non-invasive blood sugar sensors, but there are still serious obstacles to the development and mass manufacturing of these user-friendly devices due to their complexity and indirect nature of measurements (6). Despite such obstacles, recent research shows that current invasive methods are painful for patients and come with a financial burden for families. Thus, the development of non-invasive methods is necessary and interesting for the market and companies (7). Various classifications are available for non-invasive methods of measuring blood sugar (4,8-10). Among all of the available methods, transdermal measurement methods are more popular, including iontophoresis (11), bioelectric impedance (12,13), and optical methods (14-16). Optical methods are nevertheless more attractive as they come with fewer biological side effects than other methods (17,18).

Many articles and reports have been published on utilizing optical methods, but research has not ceased to propose a suitable, accurate, and affordable measurement method (19). In optical methods, the structure and optical devices are improved and the results are compared (8,20-22), or the effect of external factors (e.g., data collection from different parts of the body such as fingertips, palms, or blood vessels) is investigated (23-25).

Since reports on non-invasive measurements have covered the use of optical methods due to the high sensitivity of blood glucose (26), in this study we attempt to propose a new method based on the same spectral range but using an optical waveguide. In this article, the level of blood glucose was determined by developing a new device using near-infrared (NIR) wavelength, glass optical waveguide, and the phenomenon of evanescent waves. The light, at the contact point of the fingertip and the borehole rod, penetrates from the optical waveguide into the skin and is absorbed proportionally to the blood glucose level. The light absorption is recorded in the detector and used to measure the blood glucose.

Materials and Methods

The body's interstitial fluid has made possible the development of new technology to measure the blood glucose. The interstitial fluid contains glucose, salt, fatty acids, and minerals such as calcium, magnesium, and potassium. Hence, blood sugar can be measured by measuring the glucose of this fluid.

As a result of contacting the fingertip with the body of the borehole rod, where electromagnetic waves are reflected inside, evanescent waves penetrate from the borehole into the skin and are absorbed by the interstitial fluid. The wavelength in this research is chosen so that it is absorbed more by the interstitial fluid glucose than other elements. The electromagnetic wave rate absorption at the end of the borehole rod is investigated using a detection photodetector, and its relationship to the people's actual blood glucose level. Extrapolating this relationship, people's blood sugar can be remeasured and reestimated by experimental proofing.

Where LED is the light source consists of SMD LED with a wavelength range of 780 to

[Downloaded from ijdo.ssu.ac.ir on 2026-11-20]

[DOI: 10.18502/ijdo.v13i4.8001]

850 nm and a divergence angle of θ, PR is a glass probe rod (SiO2: 72%; 8 mm in diameter and 150 mm in length), one side of which is flat and the other side is cut at an angle of 45°, and PD is a TCS3200 photodetector (made by TAOS, U.S.A.). The detector is installed at a distance D from the cross-section of the flat side and at a height d from the central axis of the probe rod. All the assembly is inside the aluminum holder. In the central area of the aluminum holder, there is a $1.5\times1.5cm^2$ space for direct contact of the finger with the probe rod.

Given the initial cutting angle of the glass rod, the light emitted from the LED source enters the prob rod with a divergence angle θ. A large portion of photons distributed in the spatial profile of the LED output reaches the end of the probe rode due to the general reflection phenomenon. See the following structure for a better understanding.

Where θ is LED divergence angle, θ_i is the angle of irradiation, $\theta_{f'}$ is the refractive angle, $n_{1\,is}$ airrefractive index, and n_2 is average glass refractive index for the LED irradiation wavelength range. Using Snell-Descartes computational relations, it can be shown that: (1):

$$\theta_{f'} = \arcsin\left(\frac{1}{\sqrt{2}}\left[\sqrt{\left(\frac{n_2}{n_1}\right)^2 - \sin^2(\theta_i)} - \sin(\theta_i)\right]\right)$$

Equation (1) shows the refraction angle of the light output from the probe rod in terms of incident light. According to Equation (1), $\theta_{f'}$ will never be equal to zero. In simple terms, the light will not be emitted vertically from the cross-section of the glass from the end of the probe rod, and the output beam will be hollow. Due to the light scattering from glass $n_{2=}\, n_2(\lambda)$, the values of $\theta_{f'}$ will be different for various wavelengths. We can substitute different values of n_2 in Equation 1 using Sellmeier equations.

Sellmeier equations are, in fact, equations that show the refractive index in terms of wavelength. The Refractive index of a glass borehole rod depends on various factors such as its composition, transmission light wavelength, ambient temperature. Since the glass composition and the ambient temperature are constant while testing, only the transmission wavelength can be variable, which the effect of this quantity on the output data will be examined in the next section.

In this research, measurement and its errors depend on different factors such as temperature, cutting angle of the borehole, optical noise of the environment. Although the measurement of the absorption rate and the so-called output power to input power ratio is investigated in 30 seconds, and the changes of these factors in this time will not be large, the impact of these factors should be minimized to design the device. Changes in the ambient temperature of more than 10 °C within 30 seconds of finger contact with the borehole can lead to a measurement error that will not occur. The cutting angle of the borehole rod will also be checked using the Vernier scale before assembling the device. Moreover, considering the small cross-section of the fingertips contact with the borehole, the ambient light noise is minimized as much as possible, and will not have a significant effect on the measurement.

In this work, a total of 100 people of varying ages visiting a specialized laboratory for daily blood sugar sampling were randomly selected to form the statistical population. Since most patients were aimed at standard checkups and measurements, there were no blood sugar concentrations above 200 mg/dL in the data collected.

Ethical considerations

The study received ethical approval from Shahid Sadoughi University of Medical Sciences and oral consent was also obtained from all individuals and volunteers before enrolling them to study. (Ethics code: 17/1/47799).

Results

In various studies, the refractive index of glass has been obtained for different wavelengths

[Downloaded from ijdo.ssu.ac.ir on 2026-11-20]

[DOI: 10.18502/ijdo.v13i4.8001]

using Sellmeier equations and reported separately (27-31).

Figure 1 is the scatter diagram graph of glass refractive index in various wavelengths, which is plotted based on the Sellmeier equation measured by Malitson in the wavelength range of λ = 200-3725*nm* (32).

The upper and lower limits of the angle of light emitted from the probe rod depend on the angle of the incoming light (θ). Thus, θ= 0,15,30,45,60,75,90 deg, the values of the upper ($\theta_{f',\max}$) and lower ($\theta_{f',\min}$) limits were obtained using Equation 1 and the simulation in Origin Pro 8.

As demonstrated in Figure 2, with an increase in wavelength and the angle of the incoming light (θ), the lower limit of the output light ($\theta_{f',\min}$) of the probe rod decreases. For θ = *90*, the minimum irradiation of the output scattered light from the end of the probe rod is

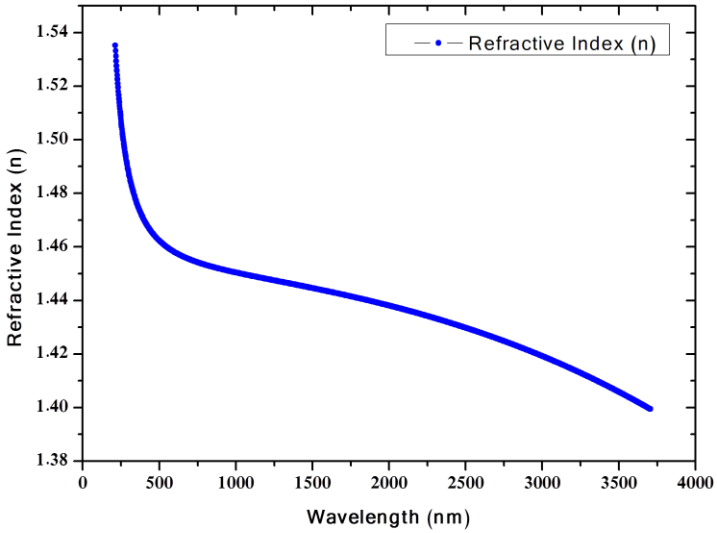


Figure 1. The scatter diagram graph of glass refractive index in wavelengths.

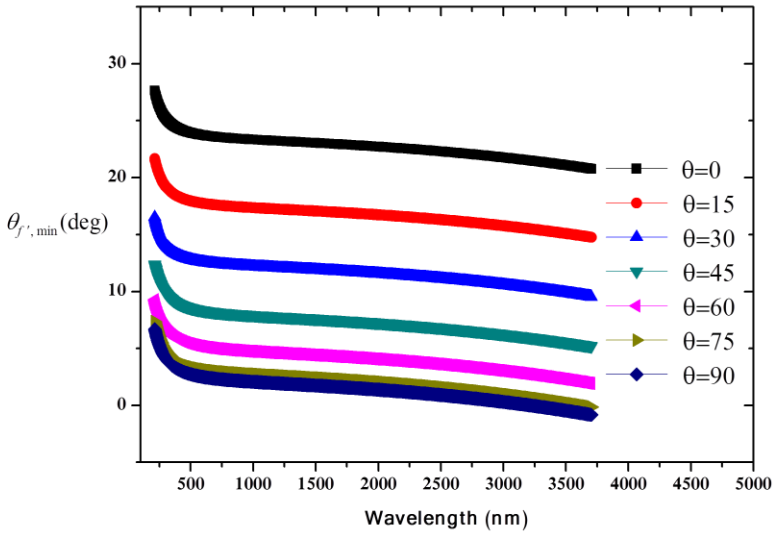


Figure 2. The lower limit of the light output angle of the probe rod for θ= 0,15,30,45,60,75,90 deg.

[Downloaded from ijdo.ssu.ac.ir on 2026-11-20]

[DOI: 10.18502/ijdo.v13i4.8001]

$\theta_{f',min}$= 0, i.e., there will no longer the output hollow beam at the end of the probe rod. The diagram in Figure 6 shows that $\theta \geq$ 75, the output light beam will no longer retain its hollow state.

Figure 3 shows the upper limit of the output light, where the value of the upper output light limit ($\theta_{f',max}$) decreases with increasing wavelength, while it increases with an increase in the angle of incoming light from the probe rod (θ). For θ = 90, or the scratch state on the edge of the probe rod, the output light will be emitted nearly tangential to the flat plate at the end of the probe rod.

According to Figures 5 and 6, it can be concluded that the beams enter the probe rod with an angle of divergence greater than zero (θ = 0), due to having larger $\theta_{f',max}$, leave the end of the probe rod with the greatest impact on the glass-air cylindrical interface and the multiplicity of the general reflection phenomenon. Therefore, such beams are more sensitive and proper for detecting and making evanescent waves. In other words, since the

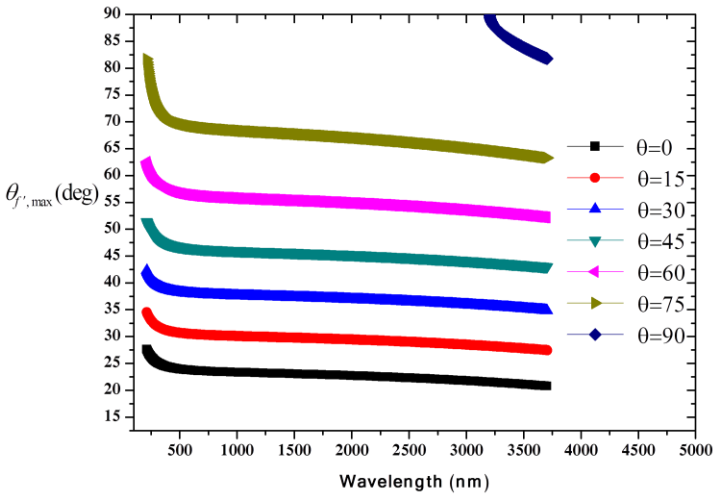


Figure 3. The upper limit of the angle of light output from the probe rod for θ= 0,15,30,45,60,75,90 deg.

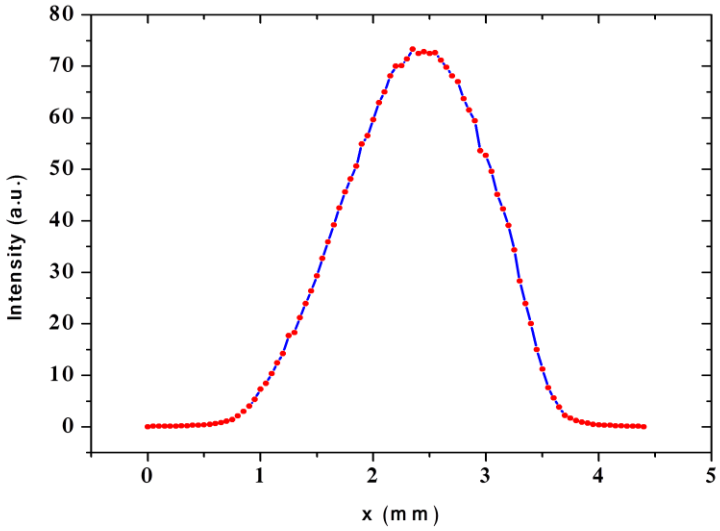


Figure 4. Spatial profile of the He-Ne laser at a distance of 3 mm from the inlet edge of the probe rod.

[Downloaded from ijdo.ssu.ac.ir on 2026-11-20]

[DOI: 10.18502/ijdo.v13i4.8001]

light output from the end of the probe rod is a mixture of incoming lights with different angles, the radius of the output light is useful for detection that has the longest optical path inside the glass rod and the greatest impact with the glass-air cylindrical interface. According to Figures 5 and 6, the larger radii of the output beam from the probe rod show the longest optical path.

Blood glucose concentration, however, is not sensitive to all wavelength ranges. As reported previously, the best wavelength for detecting blood sugar levels is within the NIR range (26). In this study, an LED source with a wavelength range of 780 to 850 nm was used for the non-invasive determination of blood glucose concentrations.

First of all, to show the accuracy of the analytical calculations, the spatial index of the output of the probe rod was measured. a He-

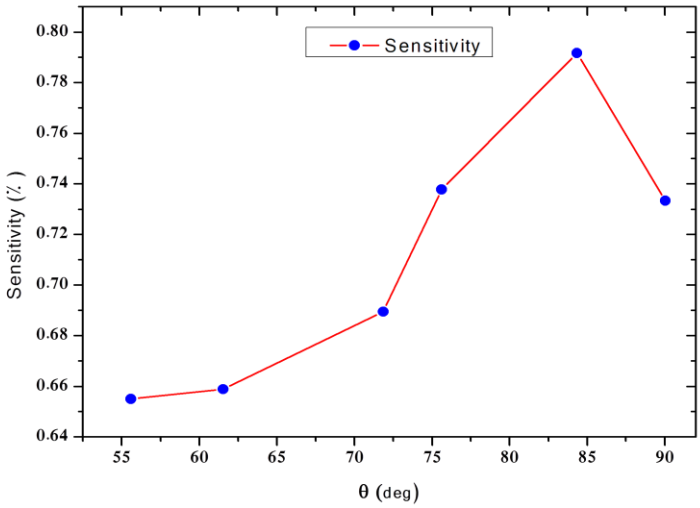


Figure 5. Experimental diagram of determining the sensitivity of a blood glucose meter in terms of changes $\theta_{d,D}$ in the displacement of the PD detector.

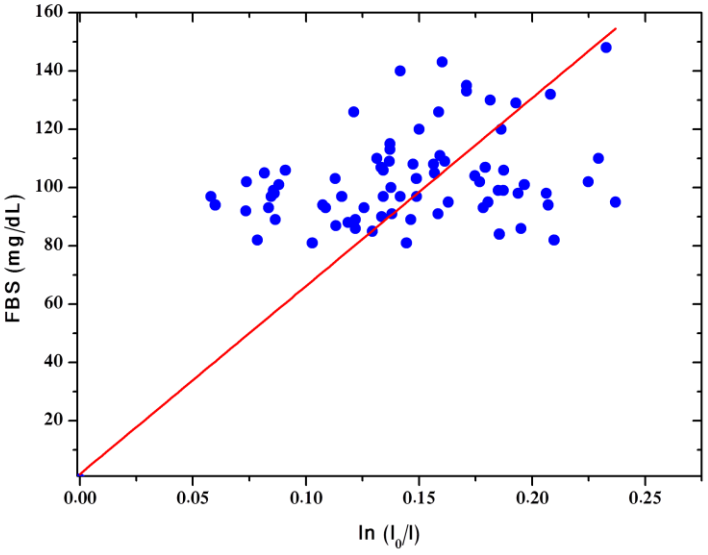


Figure 6. Experimental diagram of intravenous blood glucose determination considering the values of absorption coefficient recorded by the blood glucose meter.

[Downloaded from ijdo.ssu.ac.ir on 2026-11-20]

[DOI: 10.18502/ijdo.v13i4.8001]

Ne laser with Gaussian spatial profile, 5 mW power, and a divergence angle $\delta\theta$=1.13 *mrad* at a distance of 1300 mm from the laser output opening was used.

The laser output index was measured at a distance of 1300 mm from its outlet and 3 mm from the inlet edge of the probe rod using the optical knife-edge technique (33).

In Figure 4, the laser beam diameter was d=3.40 mm and the beam diameter at half maximum was d_{FWHM}=1.54 mm. The laser output profile from the end of the probe rod will be as follows:

Since the perforated profile is hard to reveal using the optical knife-edge technique (33), this index is swept using the required scanner (34).

The diameter of the hole in the output profile was 16.2 mm and the divergence angle was which differs from its calculated value by approximately 1 degree. This measurement shows the accuracy of analytical calculations and graphs plotted.

According to the analytical calculation and experimental results, the spatial position of the detector (PD) and the LED source in the designed sensor are of great importance. Figure 10 shows the measurement sensitivity of the designed sensor in terms of PD position. Sensitivity in Figure 5 refers to loading a completely identical wet sample on the window of the blood glucose meter and measuring the percentage of changes in output power to the initial input irradiation power in terms of changes in d and D and ultimately $\theta_{d,D}$= $\tan^{-1}$(d/D) in the position of the PD detector according to Figure 2. As demonstrated in Figure 10, the sensitivity of the detection is largely dependent on the spatial position of the PD. At larger values of d and smaller values of D, the sensitivity will improve because the detector is installed where the beams with the new path length are emitted from the end of the probe rod. Therefore, the best place for installing the PD detector in this device is at D= 0.7 mm and d= 7 mm, provided that the LED is not moved at the proximal area of the probe rod. In this

Table 1. Characteristics of the fitted line graph diagrams in the data of figure 7.

Equation	y = a + b*x	Linear	Standard error
Adj. R-Square	0.9064		
FBS	Intercept (a)	1.72932	0.72556
	Slope (b)	645.10478	10.64734

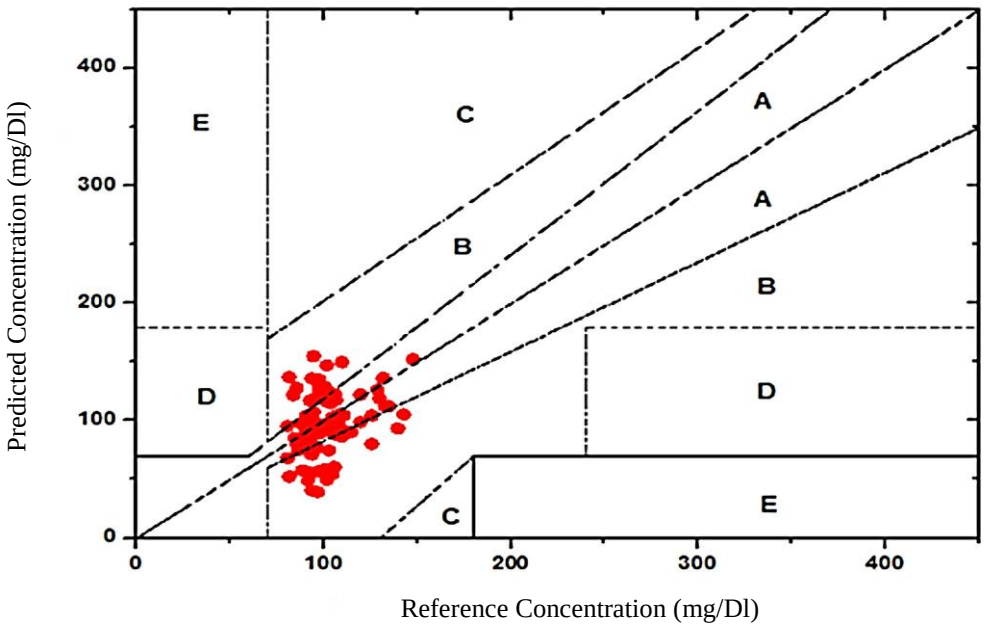


Figure 7. The Clarke error grid analysis.

[Downloaded from ijdo.ssu.ac.ir on 2026-11-20]

[DOI: 10.18502/ijdo.v13i4.8001]

research, the tip of the probe rod on the LED screen is tangent to obtain the maximum divergence angle (θ).

In this work, a total of 100 people of varying ages visiting a specialized laboratory for daily blood sugar sampling were randomly selected to form the statistical population. Since most patients were aimed at standard checkups and measurements, there were no blood sugar concentrations above 160 mg/dL in the data collected.

Before sampling, all participants were asked to hold the index finger of the right hand on the blood glucose meter for 30 seconds. The intensity of the output light was recorded before and after touching the device. Following each touch, the contact area was completely disinfected with 90% alcohol. Two minutes after measurements, blood samples were collected intravenously from participants using an autoanalyzer for standard blood glucose determination.

Figure 6 shows the relationship between intravenous blood glucose determination and the value of absorption coefficient recorded by the blood glucose meter. With linear fitting in the data presented in Figure 6, the second-order correlation coefficient of the data is equal to R-Square= 0.9064, indicating the acceptable correlation of the data.

By using the data from Table 1, we can plot the diagram of blood sugar calculated by the innovative blood glucose meter with laboratory reference data in the Clarke error grid analysis (35).

As demonstrated in Figure 7, the data measured and calculated by the new glucose monitoring device are located in areas A and B and are clinically acceptable.

Discussion

It is, however, required to consider the larger samples and statistical population to improve the accuracy as well as the measurement range. Users also come with several measurement errors which should be addressed as much as possible.

This method is much simpler than other optical methods. The FTIR or Spectrophotometer has been used in many optical methods, while this method uses generating unstable waves and a photon detector. Using Spectrophotometer systems makes it possible to examine the results for a wide wavelength range, and researchers can adjust and sensitize their results to any desired wavelength, however, only the intensity of the LED wavelength can be read in this system. Measuring the blood sugar by the designed sensor of this paper, like other methods, depends on the contact pressure of the fingertips. The measurement data by the proposed system, like other methods, are in the clinically acceptable range.

Conclusions

There are many techniques proposed for the determination of blood glucose levels. Among all of these methods, non-invasive measurements, e.g., precise optical measurements with NIR wavelengths, are popular for both users and researchers. In this study, following the literature review, a special model of NIR wavelength utilization using glass optical waveguide assisted with the phenomenon of evanescent waves was proposed. The design and manufacture of this device to enhance the accuracy of measurements were discussed both computationally and experimentally and a good agreement was observed between the results. According to the results, choosing an appropriate wavelength and the location of the LED light source and the photon detector are influential factors in improving the accuracy and sensitivity of blood glucose determination. A blood glucose meter was designed and manufactured considering all influential factors and computational and experimental results.

Then, by choosing a statistical population of 100 people of varying ages, blood sugar was measured by two standard intravenous samplings and using the innovative device proposed in this study, and the results were

[Downloaded from ijdo.ssu.ac.ir on 2026-11-20]

[DOI: 10.18502/ijdo.v13i4.8001]

compared. Experimental results showed that the values measured by the innovative device are clinically acceptable with Clark grid analysis.

For future studies, it is recommended to work with a larger statistical population and use errors diminishing trends to improve the accuracy and expand the range of measurements.

Acknowledgments

The authors thank and appreciate the efforts and cooperation of all the researchers of Shahid Sadoughi Hospital in Yazd (Iran) for their kind contributions and collaborations.

Funding

There was no funding for this research work.

Conflict of Interest

The authors declare that there is no conflict of interest regarding the publication of this paper.

References

1. Delbeck S, Vahlsing T, Leonhardt S, Steiner G, Heise HM. Non-invasive monitoring of blood glucose using optical methods for skin spectroscopy-opportunities and recent advances. Analytical and bioanalytical chemistry. 2019;411(1):63-77.
2. Pandey R, Paidi SK, Valdez TA, Zhang C, Spegazzini N, Dasari RR, et al. Noninvasive monitoring of blood glucose with Raman spectroscopy. Accounts of chemical research. 2017;50(2):264-72.
3. Klonoff DC. Noninvasive blood glucose monitoring. Diabetes care. 1997;20(3):433-7.
4. Abd Salam NA, bin Mohd Saad WH, Manap ZB, Salehuddin F. The evolution of non-invasive blood glucose monitoring system for personal application. Journal of Telecommunication, Electronic and Computer Engineering (JTEC). 2016;8(1):59-65.
5. Bruen D, Delaney C, Florea L, Diamond D. Glucose sensing for diabetes monitoring: recent developments. Sensors. 2017;17(8):1866.
6. Lin T, Gal A, Mayzel Y, Horman K, Bahartan K. Non-invasive glucose monitoring: a review of challenges and recent advances. Curr. Trends Biomed. Eng. Biosci. 2017;6(5):1-8.
7. Villena Gonzales W, Mobashsher AT, Abbosh A. The progress of glucose monitoring-A review of invasive to minimally and non-invasive techniques, devices and sensors. Sensors. 2019;19(4):800.
8. Nawaz A, Qhlckers P, Saelid S, Jacobsen M, Nadeem Akram M. Review: Non-invasive continuous blood glucose measurement techniques. J. Bioinforma. Diabetes. 2016;1(3):1-27.
9. Chivukula P, Sangeetha MS, Brindha D, Nivethitha D. Review on Blood glucose measurement techniques. International Journal of Biomedical Engineering. 2018;3(1):7-11.
10. Kavitha G, Kumar KS. Nanosensors in Blood Glucose Measurement: A Review. Indian Journal of Public Health Research & Development. 2019;10(4).
11. Lipani L, Dupont BG, Doungmene F, Marken F, Tyrrell RM, Guy RH,et al. Non-invasive, transdermal, path-selective and specific glucose monitoring via a graphene-based platform. Nature nanotechnology. 2018;13(6):504-11.
12. Kamat DK, Bagul D, Patil PM. Blood glucose measurement using bioimpedance technique. Advances in Electronics. 2014;2014.
13. Jun MH, Kim S, Ku B, Cho J, Kim K, Yoo HR, et al. Glucose-independent segmental phase angles from multi-frequency bioimpedance analysis to discriminate diabetes mellitus. Scientific reports. 2018;8(1):1-1.
14. Lane SM, Mastrototaro JJ. Development of Chemically Amplified Optical Sensors for Continuous Blood Glucose Monitoring Final Report CRADA No. TSB-1162-95. Lawrence Livermore National Lab.(LLNL), Livermore, CA (United States); 2018.
15. Kim JH, Bae HU, Kwak HS, Lee TH, Cho SU, Jeong MY. Optical blood glucose sensor based on multimode interference (MMI) fabricated by thermal imprint process. Nanoscience and Nanotechnology Letters. 2017;9(8):1222-6.
16. Chen KC, Li YL, Wu CW, Chiang CC. Glucose sensor using U-shaped optical fiber probe with gold nanoparticles and glucose oxidase. Sensors. 2018;18(4):1217.
17. Yang G, Yao XS, Su Y, Liu S, Feng T, Chen L,et al. Dermis-simulating phantom for noninvasive blood glucose sensing with OCT. InCLEO: QELS_Fundamental Science 2018 May 13 (pp. JTu2A-98). Optical Society of America.
18. Elsherif M, Hassan MU, Yetisen AK, Butt H. Hydrogel optical fibers for continuous glucose monitoring. Biosensors and Bioelectronics. 2019;137:25-32.

[Downloaded from ijdo.ssu.ac.ir on 2026-11-20]

[DOI: 10.18502/ijdo.v13i4.8001]

19. Kalidoss R, Umapathy S. An overview on the exponential growth of non-invasive diagnosis of diabetes mellitus from exhaled breath by nanostructured metal oxide Chemi-resistive gas sensors and μ-preconcentrator. Biomedical microdevices. 2020;22(1):1-9.
20. Kasahara R, Kino S, Soyama S, Matsuura Y. Noninvasive glucose monitoring using mid-infrared absorption spectroscopy based on a few wavenumbers. Biomedical optics express. 2018;9(1):289-302.
21. Liu L, Feng L, Chen H, Wang Z. Non-invasive blood glucose prediction based on spectroscopy. Investigacion Clinica. 2019;60(4):775-88.
22. Kurasawa S, Koyama S, Ishizawa H, Fujimoto K, Chino S. Verification of non-invasive blood glucose measurement method based on pulse wave signal detected by FBG sensor system. Sensors. 2017;17(12):2702.
23. Bauer A, Hertzberg O, Küderle A, Strobel D, Pleitez MA, Mäntele W. IR-spectroscopy of skin in vivo: Optimal skin sites and properties for non-invasive glucose measurement by photoacoustic and photothermal spectroscopy. Journal of biophotonics. 2018;11(1):e201600261.
24. Uwadaira Y, Ikehata A, Momose A, Miura M. Identification of informative bands in the short-wavelength NIR region for non-invasive blood glucose measurement. Biomedical optics express. 2016;7(7):2729-37.
25. Lan YT, Kuang YP, Zhou LP, Wu GY, Gu PC, Wei HJ, et al. Noninvasive monitoring of blood glucose concentration in diabetic patients with optical coherence tomography. Laser Physics Letters. 2017;14(3):035603.
26. Alam MM, Saha S, Saha P, Nur FN, Moon NN, Karim A, et al. D-care: A non-invasive glucose measuring technique for monitoring diabetes patients. InProceedings of International Joint Conference on Computational Intelligence 2020 (pp. 443-453). Springer, Singapore.
27. Tan CZ, Arndt J. Refractive index, optical dispersion, and group velocity of infrared waves in silica glass. Journal of Physics and Chemistry of Solids. 2001;62(6):1087-92.
28. Tan CZ. Determination of refractive index of silica glass for infrared wavelengths by IR spectroscopy. Journal of Non-Crystalline Solids. 1998;223(1-2):158-63.
29. Matsuoka J, Kitamura N, Fujinaga S, Kitaoka T, Yamashita H. Temperature dependence of refractive index of SiO2 glass. Journal of non-crystalline solids. 1991;135(1):86-9.
30. Ghosh G, Endo M, Iwasaki T. Temperature-dependent Sellmeier coefficients and chromatic dispersions for some optical fiber glasses. Journal of Lightwave Technology. 1994;12(8):1338-42.
31. Tan CZ, Arndt J, Xie HS. Optical properties of densified silica glasses. Physica B: Condensed Matter. 1998;252(1-2):28-33.
32. Malitson IH. Interspecimen comparison of the refractive index of fused silica. Josa. 1965;55(10):1205-9.
33. Askarbioki M, Zarandi MB, Khakshournia S, Shirmardi SP, Sharifian M. Electron beams scanning: A novel method. Nuclear Instruments and Methods in Physics Research Section A: Accelerators, Spectrometers, Detectors and Associated Equipment. 2018;894:81-6.
34. Askarbioki M, Zarandi MB, Khakshournia S, Shirmardi SP, Sharifian M. Design and fabrication of 1D and 2D optical scanner for electron beams using color centre generation. Journal of Instrumentation. 2018;13(12):T12003.
35. Clarke WL. The original Clarke error grid analysis (EGA). Diabetes technology & therapeutics. 2005;7(5):776-9.

[Downloaded from ijdo.ssu.ac.ir on 2026-11-20]

[DOI: 10.18502/ijdo.v13i4.8001]